JACS
JOURNAL OF THE AMERICAN CHEMICAL SOCIETY

Article

pubs.acs.org/JACS

Elucidating the Molecular Function of Human BOLA2 in GRX3-Dependent Anamorsin Maturation Pathway

Lucia Banci,*[,†,‡] Francesca Camponeschi,[†,‡] Simone Ciofi-Baffoni,*[,†,‡] and Riccardo Muzzioli[†,‡]

[†]Magnetic Resonance Center CERM, University of Florence, Via Luigi Sacconi 6, 50019, Sesto Fiorentino, Florence, Italy
[‡]Department of Chemistry, University of Florence, Via della Lastruccia 3, 50019 Sesto Fiorentino, Florence, Italy

Supporting Information

ABSTRACT: In eukaryotes, the interaction between members of the monothiol glutaredoxin family and members of the BolA-like protein family has been involved in iron metabolism. To investigate the still unknown functional role of the interaction between human glutaredoxin-3 (GRX3) and its protein partner BOLA2, we characterized at the atomic level the interaction of apo BOLA2 with the apo and holo states of GRX3 and studied the role of BOLA2 in the GRX3-dependent anamorsin maturation pathway. From these studies, it emerged that apo GRX3 and apo BOLA2 form a heterotrimeric complex, composed by two BOLA2 molecules and one GRX3 molecule. This complex is able to bind two $[2Fe\text{-}2S]^{2+}$ clusters, each being bridged between a BOLA2 molecule and a monothiol glutaredoxin domain of GRX3, and to transfer both $[2Fe\text{-}2S]^{2+}$ clusters to apo anamorsin producing its mature holo state. Collectively, the data suggest that the heterotrimeric complex can work as a $[2Fe\text{-}2S]^{2+}$ cluster transfer component in cytosolic Fe/S protein maturation pathways.

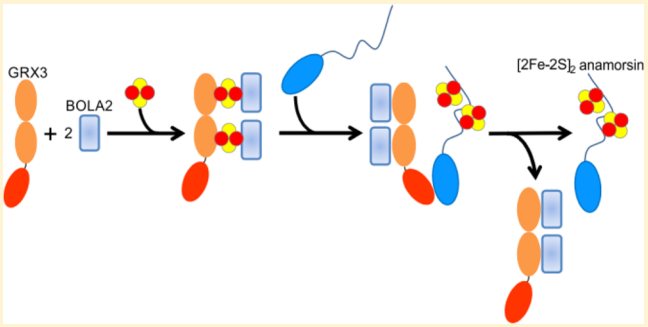

INTRODUCTION

In eukaryotes, the biosynthetic pathways responsible for the maturation of Fe/S proteins is a complex, multistep process involving more than 30 different proteins.[1] As a result, atomic level studies are vital to fully unravel the molecular function of each single player in the Fe/S protein maturation process. In this work, we characterized at the atomic level the interaction between human glutaredoxin-3 (GRX3) and its protein partner BOLA2 and identified a possible role for BOLA2 in the GRX3-dependent anamorsin maturation pathway.

The functional role of eukaryotic monothiol glutaredoxins (Grx) has been largely studied in *Saccharomyces cerevisiae*, which encodes three CysGlyPheSer(CGFS)-type monothiol Grx homologues, Grx3, Grx4, and Grx5.[2−4] Grx5 is a single domain protein, located in the mitochondrial matrix, which binds a [2Fe-2S] cluster ligated by two protein molecules, each providing a cysteine ligand, and by two glutathione molecules, each providing a further cysteine ligand.[5,6] Grx5 has been shown to participate in the mitochondrial iron−sulfur (Fe/S) cluster (ISC) assembly machinery, acting, in its holo-homodimeric state, as a donator of a [2Fe-2S] cluster to partner apo-proteins.[7,8] Grx3 and Grx4 are located in the cytoplasm, and each consists of a N-terminal thioredoxin (Trx) domain, with no Trx-related activity,[9,10] and of a glutaredoxin domain capable of binding a [2Fe-2S] cluster through protein dimerization and glutathione binding,[11] in the same way as Grx5 does. Grx3 and Grx4 have been linked to iron regulation through their binding to the transcriptional activator Aft1/2, which regulates iron uptake in yeast.[12−14] Specifically, to perform this regulatory function, Grx3 (or Grx4) needs to be complexed with the BolA-like protein Fra2, forming a [2Fe-2S]-bridged heterodimeric complex,[11,15] which, at variance with the holo-homodimeric species, can transfer the cluster to the iron-responsive transcription factor Aft2.[16] Based on this information on yeast, holo-heterodimeric Grx/BolA complexes have been generally linked to iron homeostasis regulation, while holo-homodimeric Grx complexes have been related to Fe/S protein biogenesis.[17] Recently, it has been also shown that double depletion of yeast Grx3/4 specifically impaired all iron-requiring reactions in the cytosol, in mitochondria, and in the nucleus, including the synthesis of Fe/S clusters, of heme, and of di-iron centers.[9] These data suggest that holo-homodimeric cytoplasmatic Grxs species can also function in intracellular iron trafficking.

In humans, two monothiol Grxs are present, GRX3 and GRX5.[2,18] GRX5 is located in mitochondria essentially performing the same function as the yeast Grx5 homologue, i.e., it acts as a [2Fe-2S] cluster transfer protein in the ISC machinery.[19,20] GRX3 consists of three domains: one N-terminal Trx domain and two Grx domains, each able to bind a glutathione-coordinated [2Fe-2S] cluster via protein dimerization.[21,22] GRX3 is located in the cytosol, and similarly to what was found for yeast Grx3/Grx4, the molecular function of its holo-homodimeric state ($[2Fe\text{-}2S]_2$ $GRX3_2$) has been associated with intracellular iron trafficking, being responsible

Received: October 9, 2015
Published: November 27, 2015

DOI: 10.1021/jacs.5b10592
J. Am. Chem. Soc. 2015, 137, 16133−16143

for iron redistribution to virtually all iron-binding proteins or iron-dependent pathways in the cell.[23] Recently, we proposed that human GRX3 is an active component of the cytosolic Fe/S cluster assembly (CIA) machinery, as its homodimeric [2Fe-2S]$_2$ GRX3$_2$ form is able to mature the cytosolic [2Fe-2S]-binding protein anamorsin, an essential component of the CIA machinery.[24] The CIA machinery is responsible for the maturation of cytosolic and nuclear Fe/S proteins performing key functions in metabolic catalysis, iron regulation, protein translation, DNA synthesis, and DNA repair.[25,26] Therefore, the cellular function of GRX3 in maturing the CIA component anamorsin indirectly affects several crucial life processes.

Similarly to yeast, GRX3 can form a holo-hetero complex with a BolA-like protein, the cytosolic BOLA2.[21] However, while the yeast Grx3/4 forms a [2Fe-2S]-bridged heterodimer with a Fra2 molecule, the human GRX3 forms a [2Fe-2S]-bridged heterotrimer with two BOLA2 molecules ([2Fe-2S]$_2$ GRX3-BOLA2$_2$). Since there is no human ortholog of the transcription factor Aft1, being indeed cellular iron homeostasis in humans regulated at the RNA-level by the Iron Regulatory Proteins 1 and 2,[27] [2Fe-2S]$_2$ GRX3-BOLA2$_2$ heterotrimers cannot be involved in the same [2Fe-2S] cluster transfer pathway found in yeast to regulate iron homeostasis. Although other functions of the [2Fe-2S]$_2$ GRX3-BOLA2$_2$ heterotrimer in human cells might be possible, it seems conceivable that this complex takes a role in iron metabolism given that (i) [2Fe-2S]-bridged Grx3−BolA2 interaction is conserved from *S. cerevisiae* to humans,[17] (ii) human GRX3 binds iron *in vivo*,[22] and (iii) human GRX3 partially rescues the growth defects and iron accumulation in the *S. cerevisiae grx3Δgrx4Δ* mutant, suggesting that human GRX3 partially can complement the functions of yeast Grx3 and Grx4 in iron homeostasis.[28]

In this work we have characterized *in vitro* the interaction of apo BOLA2 with the apo and holo states of GRX3 and investigated the role of BOLA2 in the GRX3-dependent anamorsin maturation pathway.

EXPERIMENTAL SECTION

Protein Production. The cDNA coding for human BOLA2 (UniProtKB/Swiss-Prot: Q9H3K6) was acquired from Life technologies. BOLA2 gene was amplified by PCR and subsequently inserted into the pET21a vector using the restriction enzymes NdeI and BanHI. BL21(DE3) gold competent *Escherichia coli* cells (Stratagene, La Jolla, CA) were transformed with the obtained plasmid, and cells were grown in LB or minimal media (with $(^{15}NH_4)_2SO_4$ and/or [^{13}C]-glucose) containing 1 mM ampicillin at 37 °C under vigorous shaking up to a cell OD_{600} of 0.6. Protein expression was induced by adding 0.5 mM IPTG, and cells were grown for 4 h at 25 °C. Cells were harvested by centrifugation at 7500*g* and resuspended in lysis buffer (25 mM MES pH 6 containing 0.01 mg/mL DNAase, 0.01 mg/mL lysozyme, 1 mM $MgSO_4$, 0.5 mM EDTA, and 5 mM DTT). Cell disruption was performed on ice by sonication, and the soluble extract, obtained by ultracentrifugation at 40000*g*, was loaded on HiTrap SP FF column (GE Healthcare). BOLA2 protein was eluted with 25 mM MES pH 6, 1 M NaCl and 5 mM DTT, concentrated with Amicon Ultra-15 Centrifugal Filter Units with a MWCO of 3 kDa (Millipore), and the buffer exchanged by PD10 desalting column in 50 mM phosphate buffer pH 7, 5 mM DTT and 5 mM GSH.

Various constructs of human GRX3 (full-length protein, Trx, and GRX3(GrxA/B) constructs in their apo and/or [2Fe-2S]-bound forms) were obtained following previously reported procedures.[24] [2Fe-2S]$_2$ GRX3$_2$ was obtained by chemical reconstitution following a previously reported procedure.[24]

Biochemical and UV−vis, CD, EPR Spectroscopic Methods. The aggregation state of isolated apo and holo proteins and of protein mixtures was analyzed using analytical gel filtration on Superdex 75 HR 10/30 and Superdex 200 10/300 increase columns (Amersham Bioscience), calibrated with gel filtration marker calibration kit, 6500−66000 Da (Sigma-Aldrich), to obtain the apparent molecular masses of the detected species. Purified samples in degassed phosphate buffer 50 mM pH 7, 5 mM DTT, and 5 mM GSH were loaded on the column pre-equilibrated with degassed 50 mM phosphate buffer pH 7, 5 mM GSH, and 5 mM DTT. Elution profiles were recorded at 280 nm with a flow rate of 0.5 mL/min for Superdex 75 HR 10/30 column and 0.75 mL/min for Superdex 200 10/300 increase column.

UV−vis and CD spectra were anaerobically acquired on a Cary 50 Eclipse spectrophotometer and JASCO J-810 spectropolarimeter, respectively, in degassed 50 mM phosphate buffer pH 7, 5 mM GSH, and 5 mM DTT.

EPR spectra of the 1:4 [2Fe-2S]$_2$ GRX3$_2$-apo BOLA2 mixture and of the chemically reconstituted [2Fe-2S]$_2$ GRX3-BOLA2$_2$ heterotrimeric complex were recorded after the anaerobic reduction of the cluster by stoichiometric addition of sodium dithionite and immediate freezing of the protein solution in liquid nitrogen. EPR spectra were acquired in degassed 50 mM phosphate buffer pH 7, 5 mM GSH, 5 mM DTT, and 10% glycerol at 45 K, using a Bruker Elexsys E500 spectrometer working at a microwave frequency of ca. 9.45 GHz, equipped with a SHQ cavity and a continuous flow He cryostat (ESR900, Oxford instruments) for temperature control. Acquisition parameters were as following: microwave frequency, 9.640928 GHz; microwave power, 5 mW; modulation frequency, 100 kHz; modulation amplitude, 2.0 G; acquisition time constant, 163.84 ms; number of points 1024; number of scans 8; field range 500−6000 G or 2300−4300 G.

The iron and inorganic sulfur content and the protein concentration were estimated following standard chemical assays as already reported.[29]

NMR Spectroscopy. Standard ^{1}H-detected triple-resonance NMR experiments for backbone resonance assignment were recorded on 1 mM ^{13}C, ^{15}N-labeled samples (apo forms of GRX3(GrxA/B) and BOLA2) in degassed 50 mM phosphate buffer pH 7, 5 mM DTT, and 5 mM GSH at 298 K, using Bruker AVANCE 500 and 700 MHz spectrometers. ^{15}N heteronuclear relaxation experiments were performed on ^{15}N-labeled apo BOLA2 and on ^{15}N-labeled apo GRX3(GrxA/B) in the presence and in the absence of 2 equiv of unlabeled apo BOLA2, in degassed 50 mM phosphate buffer pH 7, 5 mM DTT, and 5 mM GSH at 298 K, to measure ^{15}N backbone longitudinal (R_1) and transverse (R_2) relaxation rates and heteronuclear ^{15}N{^{1}H} NOEs. All NMR data were processed using the Topspin software package and were analyzed with the program CARA.

An apparent dissociation constant (K_d) for the interaction between apo GRX3(GrxA/B) and apo BOLA2 proteins, in degassed 50 mM phosphate buffer pH 7, 5 mM DTT at 298 K, was obtained by plotting the average chemical shift differences δ_{av} (i.e., $(((\Delta H)^2 + (\Delta N/5)^2)/2)^{1/2}$, where ΔH and ΔN are chemical shift differences for backbone amide ^{1}H and ^{15}N nuclei, respectively) of five well-resolved backbone NH signals of ^{15}N-labeled GRX3(GrxA/B) and of six well resolved backbone NH signals of ^{15}N-labeled BOLA2, as a function of BOLA2 and GRX3(GrxA/B) concentrations, respectively. These data were then fitted to a simple two-component model and averaged to obtain the final K_d value.[30,31]

Protein−Protein Interaction and Cluster Transfer. Apo GRX3 (or apo GRX3(GrxA/B))-apo BOLA2 interaction was investigated by ^{1}H−^{15}N HSQC NMR spectra, titrating ^{15}N-labeled apo forms of GRX3 or GRX3(GrxA/B) with unlabeled apo BOLA2, and ^{15}N-labeled apo BOLA2 with unlabeled apo forms of GRX3 or GRX3(GrxA/B), in degassed 50 mM phosphate buffer pH 7, 5 mM GSH, and 5 mM DTT containing 10% (v/v) D_2O at 298 K. Spectral changes were monitored upon the addition of increasing amounts of the unlabeled partner. NMR data were analyzed with CARA program and plotted following standard procedures.

To follow changes in cluster coordination upon interaction between [2Fe-2S]$_2$ GRX3$_2$ and apo BOLA2, [2Fe-2S]$_2$ GRX3$_2$ was incubated under anaerobic conditions with increasing concentrations of apo BOLA2 up to a 1:4 protein ratio, in degassed 50 mM phosphate buffer

DOI: 10.1021/jacs.5b10592
J. Am. Chem. Soc. 2015, 137, 16133−16143

pH 7, 5 mM GSH, and 5 mM DTT. UV−vis, EPR, and CD spectra were then recorded as described above and compared with those collected on a $[2Fe\text{-}2S]_2$ GRX3-BOLA2$_2$ complex, which was obtained by chemically reconstituting a 1:2.5 apo GRX3-apo BOLA2 mixture following a previously reported procedure.[24] Protein−protein interaction between $[2Fe\text{-}2S]_2$ GRX3$_2$ and apo BOLA2 was investigated by $^1H-^{15}N$ HSQC NMR spectra performed on ^{15}N-labeled $[2Fe\text{-}2S]_2$ GRX3$_2$ titrated with unlabeled apo BOLA2 and on ^{15}N-labeled apo BOLA2 titrated with unlabeled $[2Fe\text{-}2S]_2$ GRX3$_2$. Spectral changes were monitored and analyzed upon the addition of increasing amounts of the unlabeled partner.

The chemically reconstituted $[2Fe\text{-}2S]_2$ GRX3-BOLA2$_2$ complex was titrated under anaerobic conditions with increasing concentrations of apo anamorsin up to a 1:1 protein ratio in degassed 50 mM phosphate buffer pH 7, 5 mM GSH, and 5 mM DTT. Cluster transfer and the protein−protein interaction were followed by UV−vis and CD spectroscopy and analytical gel filtration chromatography, respectively.

RESULTS

Interaction of apo GRX3 with apo BOLA2. Full-length BOLA2 protein was overexpressed in *E. coli* cells and purified in its apo form. Analytical gel filtration and ^{15}N NMR relaxation data (Supporting Information Figure S1), which provided an molecular reorientational correlation time of 6.9 ± 0.23 ns, showed that the purified apo protein is monomeric. Purified apo BOLA2 was unable to bind Fe/S clusters when a chemical reconstitution approach[29] was applied.

To investigate the interaction between the apo forms of GRX3 and BOLA2, chemical shift changes of backbone NHs were followed by $^1H-^{15}N$ HSQC NMR experiments upon titration of ^{15}N-labeled apo GRX3 with unlabeled apo BOLA2, and of ^{15}N-labeled apo BOLA2 with unlabeled apo GRX3, in the presence of 5 mM GSH and 5 mM DTT. Chemical shift variations, which were in a fast/intermediate exchange regime on the NMR time scale, were observed in the $^1H-^{15}N$ HSQC maps of GRX3 for the backbone NHs of both Grx domains, when increasing amounts of unlabeled BOLA2 were added up to a 1:2 GRX3-BOLA2 molar ratio, while no significant effects were observed on the backbone NHs of the Trx domain of GRX3 (Figure 1A). These chemical shift changes occur simultaneously on both Grx domains, thus indicating that BOLA2 does not have a preferential interaction toward one of the two Grx domains (Figure 1A, inset). Similarly, chemical shift variations in a fast/intermediate exchange regime on the NMR time scale were observed in the $^1H-^{15}N$ HSQC maps of BOLA2 when increasing amounts of unlabeled GRX3 were added up to a 1:2 GRX3-BOLA2 molar ratio (Figure 1B).

The interaction between apo BOLA2 and apo GRX3 was also followed by analytical gel filtration chromatography, performed on protein mixtures with different apo GRX3 and apo BOLA2 ratios (Figure 2A). The formation of two peaks was observed by adding apo BOLA2 to apo GRX3 up to a 1:2 GRX3-BOLA2 ratio: (i) a peak with an apparent molecular mass of 70.4 kDa, predominant at 1:1 protein ratio; (ii) a peak with an apparent molecular mass of 74.3 kDa, predominant at 1:2 protein ratio (Figure 2A). These results indicated that apo GRX3 forms a heterodimeric complex with apo BOLA2 at the 1:1 protein ratio (the 70.4 kDa value matches indeed with the sum of the apparent molecular masses of apo GRX3 and apo BOLA2), which then evolves, upon addition of a further equivalent of apo BOLA2, to form a species which has an apparent molecular mass (74.3 kDa) intermediate between that of the heterodimeric complex (70.4 kDa) and that of an apo heterotrimeric complex formed by two BOLA2 molecules and

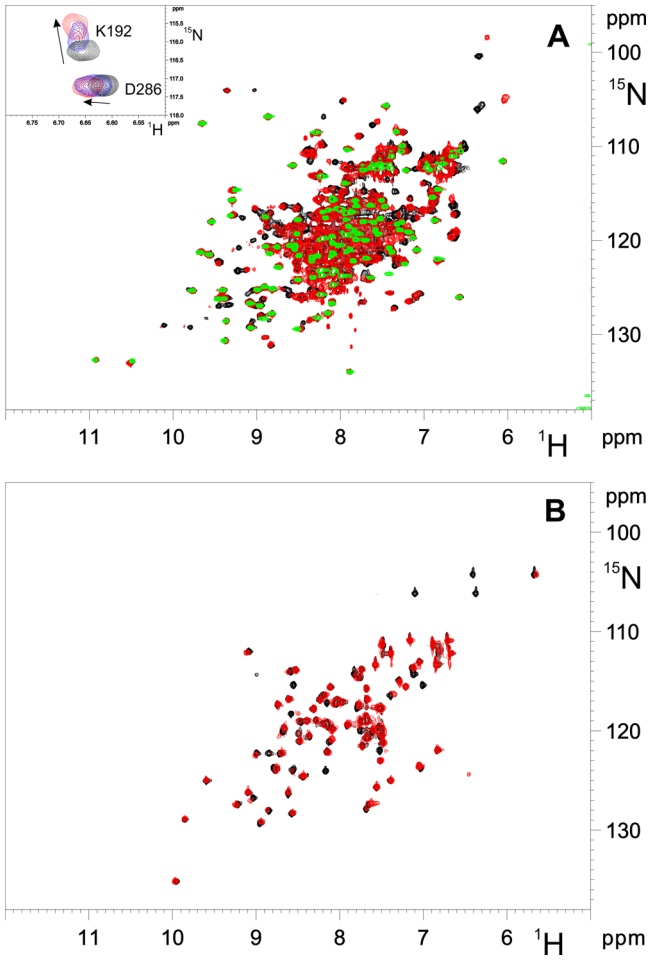

Figure 1. Apo GRX3 interacts with apo BOLA2. (A) Overlay of $^1H-^{15}N$ HSQC spectra of ^{15}N-labeled apo GRX3 (black), of ^{15}N-labeled Trx domain of GRX3 (green), and of a 1:2 mixture of ^{15}N-labeled apo GRX3 and unlabeled apo BOLA2 (red). The chemical shift changes of two backbone NHs belonging to GrxA and GrxB domains, K192 and D286, respectively, are reported in the inset for ^{15}N-labeled apo GRX3 (black), for 1:1 (blue) and 1:2 (red) mixtures of ^{15}N-labeled apo GRX3 and unlabeled apo BOLA2. (B) Overlay of $^1H-^{15}N$ HSQC spectra of ^{15}N-labeled apo BOLA2 (black) and of a 1:2 mixture of unlabeled apo GRX3 and ^{15}N-labeled apo BOLA2 (red).

one GRX3 molecule (82 kDa, obtained by the sum of the apparent molecular masses of apo GRX3 and two molecules of apo BOLA2). The presence of this peak with an intermediate apparent molecular mass can be a consequence of the applied gel filtration conditions, which determined, indeed, the presence of a fast exchange equilibrium between the heterodimeric and heterotrimeric complexes. Therefore, we performed the analytical gel filtration chromatography using a different column, i.e., Superdex 75 HR 10/30, and it resulted that apo GRX3 protein interacts with apo BOLA2 forming a peak with an apparent molecular mass of 76.8 kDa predominant at 1:2.5 GRX3-BOLA2 protein ratio (Figure 2B). This value essentially corresponds to the sum of the apparent molecular masses of apo GRX3 (52.7 kDa) and two molecules of apo BOLA2 (11.1 kDa) (Figure 2B), thus definitively indicating the formation of the apo GRX3-BOLA2$_2$ heterotrimeric complex.

DOI: 10.1021/jacs.5b10592
J. Am. Chem. Soc. 2015, 137, 16133−16143

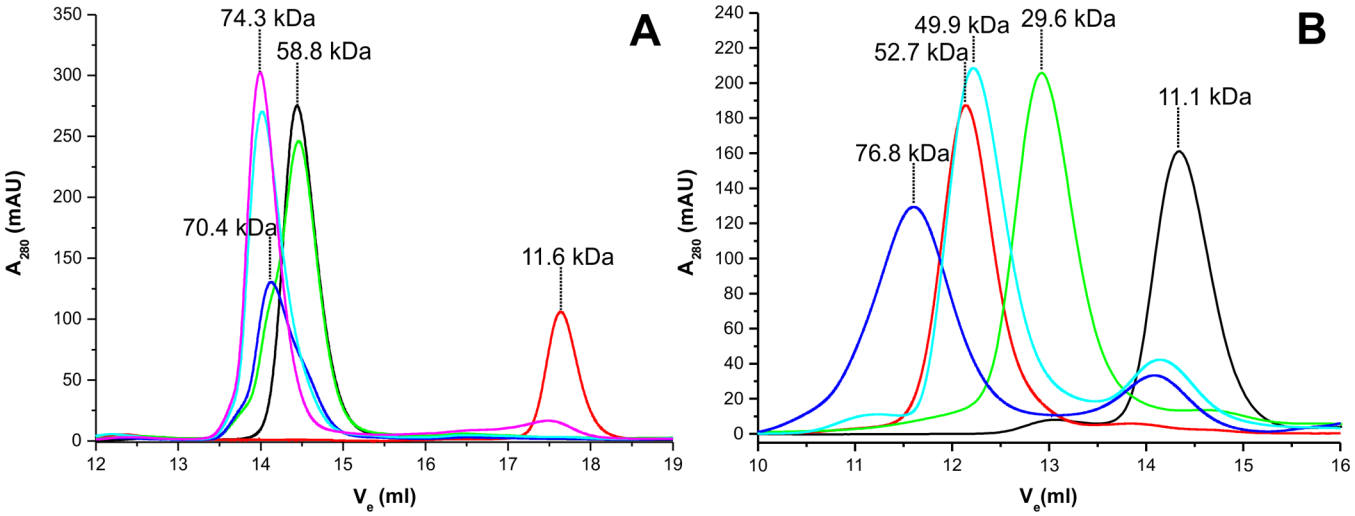

Figure 2. Apo GRX3 and apo BOLA2 form a heterotrimeric 1:2 complex. (A) Analytical gel filtration (Superdex 200 10/300 increase column) chromatograms of BOLA2 and GRX3 proteins in their apo states and of their protein mixtures. Black line: apo GRX3; red line: apo BOLA2; green line: 1:0.5 mixture of apo GRX3 and apo BOLA2; blue line: 1:1 mixture of apo GRX3 and apo BOLA2; cyan line: 1:1.5 mixture of apo GRX3 and apo BOLA2; magenta line: 1:2 mixture of apo GRX3 and apo BOLA2. The apparent molecular masses are reported at the top of each chromatographic peak. (B) Analytical gel filtration (Superdex 75 HR 10/30 column) chromatograms of isolated BOLA2, GRX3(GrxA/B) and GRX3 proteins in their apo states and of their protein mixtures. Black line: apo BOLA2; red line: apo GRX3; green line: apo GRX3(GrxA/B); cyan line: 1:2.5 mixture of apo GRX3(GrxA/B) and apo BOLA2; blue: 1:2.5 mixture of apo GRX3 and apo BOLA2. The apparent molecular masses are reported at the top of each chromatographic peak.

Since the Trx domain is not involved in the interaction between apo BOLA2 and apo GRX3, we produced a two-domain construct containing the GrxA and GrxB domains only, (GRX3(GrxA/B)), to map, by solution NMR, the residues involved in the formation of the heterotrimeric complex. With this shorter construct, the chemical shift data analysis was indeed simplified by the reduction of NMR signal overlap and broadening due to the reduced protein size. We titrated ^{15}N-labeled BOLA2 with unlabeled GRX3(GrxA/B) and ^{15}N-labeled GRX3(GrxA/B) with unlabeled BOLA2 and followed the chemical shift changes of backbone NHs via ^{1}H−^{15}N HSQC experiments. Chemical shift variations are in a fast/intermediate exchange regime on the NMR time scale in both titrations, as it occurs for the apo GRX3−apo BOLA2 interaction. By fitting the chemical shifts to a simple two-component model,[30,31] an apparent dissociation constant of 25 ± 15 μM was obtained (Figure 3A,B insets).

The ^{1}H−^{15}N HSQC signals of the final protein mixture, i.e., 1:2 ^{15}N-labeled apo GRX3(GrxA/B)-apo BOLA2, well superimposed with the corresponding signals of a 1:2 apo ^{15}N-labeled GRX3-apo BOLA2 mixture, indicating that the same complex involving the same interacting region was present in solution in the two mixtures, and confirming that Trx domain has no specific role in the protein−protein recognition between apo GRX3 and apo BOLA2 (Supporting Information Figure S2). Comparing the ^{1}H−^{15}N HSQC map of the final apo GRX3(GrxA/B)-apo ^{15}N-labeled BOLA2 mixture with that of ^{15}N-labeled BOLA2 (Figure 3B), 15 signals of BOLA2 experienced significant chemical shift variations and two NH signals broadened beyond detection (Figure 4A).

In the reverse titration, when detecting ^{15}N-labeled GRX3-(GrxA/B) (Figure 3B), 15 NH signals broadened beyond detection and 21 NH signals experienced chemical shift variations in the ^{1}H−^{15}N HSQC spectrum of the final 1:2 GRX3(GrxA/B)-BOLA2 mixture once compared with that of ^{15}N-labeled GRX3(GrxA/B) (Figure 4B).

Once the affected residues are mapped on the structural model of apo BOLA2 (calculated with MODELER 9.15 software using the solution structure of apo BOLA2 from *Mus musculus*[32] as template with a 87% sequence identity) and on the crystal structures of the apo form of the single GrxA (PDB ID 3ZYW) and GrxB (PDB ID 2YAN) domains of GRX3, well-defined interacting regions were identified on both proteins. On BOLA2 side, it comprises helix α3 and the following strand β3, containing His 68, a ligand of the [2Fe-2S]$^{2+}$ cluster[21] (Figure 4A). On each GrxA and GrxB domain, the interacting surface involves helices α2 and α3, strand β4, and the surrounding loops and comprises the Cys ligand of the [2Fe-2S]$^{2+}$ bound cluster[21] (Figure 4B).

^{15}N backbone NMR relaxation experiments, performed on ^{15}N-labeled apo GRX3(GrxA/B) in absence or in the presence of 2 equiv of apo BOLA2, showed an increase in the molecular reorientational correlation time from 12.0 ± 1.2 ns (consistent with a monomeric state of GRX3(GrxA/B) in solution) to 27.7 ± 4.5 ns. This increase is consistent with the formation of a 1:2 GRX3(GrxA/B)-BOLA2 protein complex, being the molecular reorientational correlation time of apo BOLA2 6.9 ± 0.23 ns. This result is in agreement with the analytical gel filtration data collected with a Superdex 75 HR 10/30 column (Figure 2B), which showed the formation of a peak with an apparent molecular mass of 49.9 kDa in the chromatogram of the protein mixture, which essentially corresponds to the sum of the apparent molecular masses of apo GRX3(GrxA/B) (29.6 kDa) and two molecules of apo BOLA2 (11.1 kDa).

Interaction of [2Fe-2S]$_2$ GRX3$_2$ with apo BOLA2. The interaction of apo BOLA2 with the holo-dimeric form of GRX3, i.e., [2Fe-2S]$_2$ GRX3$_2$, was characterized by UV−vis, CD, EPR, NMR, and analytical gel filtration. Upon stepwise additions of apo BOLA2 to [2Fe-2S]$_2$ GRX3$_2$, the absorbance peaks typical of the oxidized [2Fe-2S]$^{2+}$ clusters bound to GRX3 disappeared in the UV−vis and CD spectra and new absorbance peaks appeared. The final spectra (Figure 5A,B) at a

DOI: 10.1021/jacs.5b10592
J. Am. Chem. Soc. 2015, 137, 16133−16143

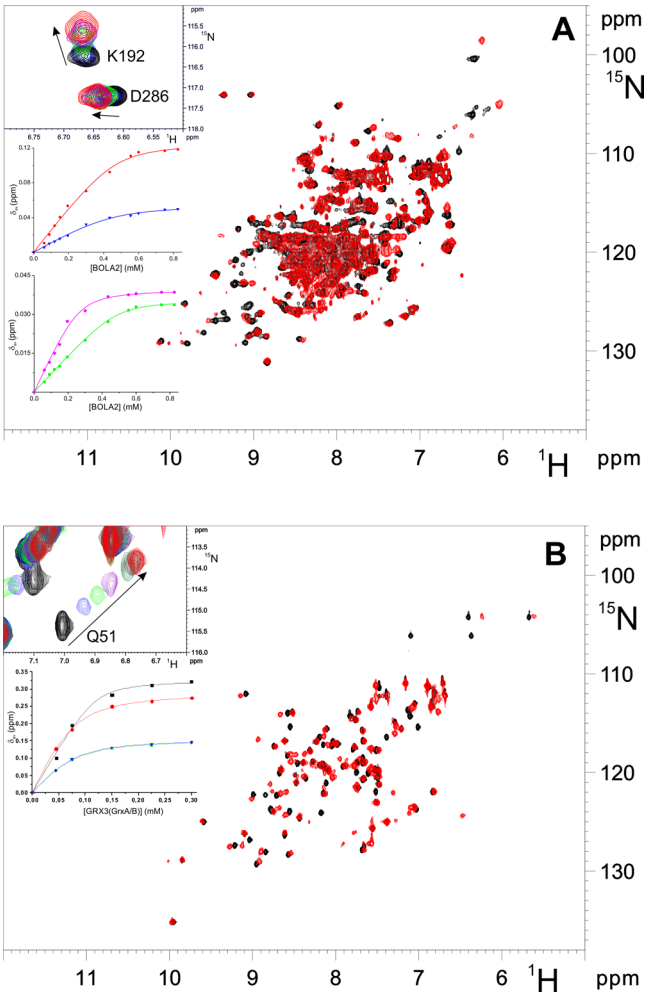

Figure 3. GrxA and GrxB domains interact with apo BOLA2. (A) Overlay of ^{1}H−^{15}N HSQC spectra of ^{15}N-labeled apo GRX3(GrxA/B) (black) and of a 1:2 mixture of ^{15}N-labeled apo GRX3(GrxA/B) and unlabeled apo BOLA2 (red). In the inset, a zoom of ^{1}H−^{15}N HSQC spectra on the K192 and D286 backbone NH signals is reported for ^{15}N-labeled apo GRX3(GrxA/B) (black) and for 1:0.5 (blue), 1:1 (green), 1:1.5 (violet), and 1:2 (red) mixtures of ^{15}N-labeled apo GRX3(GrxA/B) and unlabeled apo BOLA2. The inset also shows the δ_{av} changes measured for T199 (red circles) and Q202 (blue triangles) in the GrxA domain of GRX3(GrxA/B) and of K245 (green squares) and F263 (magenta circles) in the GrxB domain of GRX3(GrxA/B) as a function of apo BOLA2 concentration. Solid lines show the fitting curves. (B) Overlay of ^{1}H−^{15}N HSQC spectra of ^{15}N-labeled apo BOLA2 (black) and of a 2:1 mixture of ^{15}N-labeled apo BOLA2 and unlabeled apo GRX3(GrxA/B) (red). In the inset, a zoom of ^{1}H−^{15}N HSQC spectra on the Q51 backbone NH signal is reported for ^{15}N-labeled apo BOLA2 (black) and for the 0.1:1 (blue), 0.15:1 (green), 0.25:1 (violet), 0.5:1 (dark green), 0.75:1 (gray), 1:1 (brown), and 2:1 (red) mixtures of unlabeled apo GRX3(GrxA/B) and ^{15}N-labeled apo BOLA2. The inset also shows the δ_{av} changes measured for the L50 (black squares), Q51 (red circles), V56 (green up triangles), and N57 (blue down triangles) residues of BOLA2 as a function of apo GRX3(GrxA/B) concentration. Solid lines show the fitting curves.

1:4 $[2Fe\text{-}2S]_2$ $GRX3_2$-BOLA2 ratio are very similar to that of the holo complex obtained by chemically reconstituting apo GRX3-$BOLA2_2$ with two $[2Fe\text{-}2S]^{2+}$ clusters ($[2Fe\text{-}2S]_2$ GRX3-$BOLA2_2$, hereafter), as assessed by iron and acid-labile sulfide chemical analysis (Fe and acid-labile *S* values, reported as mol Fe or S per mol of trimer, are 3.8 ± 0.1 and 3.9 ± 0.1, respectively).

The 1:4 protein−protein ratio is needed to fully saturate the four Grx domains present in the dimeric $[2Fe\text{-}2S]_2$ $GRX3_2$ complex with BOLA2 molecules. The final mixture containing $[2Fe\text{-}2S]_2$ $GRX3_2$ and apo BOLA2 at a 1:4 molar ratio was EPR silent, as expected for the presence of a $S = 0$ ground state of oxidized $[2Fe\text{-}2S]^{2+}$ clusters. Upon chemical reduction with sodium dithionite, the EPR signal of a reduced $[2Fe\text{-}2S]^{+}$ protein-bound cluster is observed with *g* values of 2.01, 1.91, and ∼1.87 (g_{av} ∼ 1.93), which are the same as those observed on the chemically reconstituted heterotrimeric $[2Fe\text{-}2S]_2$ GRX3-$BOLA2_2$ complex upon sodium dithionite reduction (Supporting Information Figure S3). Analytical gel filtration chromatography, performed with a Superdex 75 HR 10/30 column on the same final mixture, showed the presence of a main peak with an apparent molecular mass of 73.2 kDa, which is very close to the sum of the apparent molecular masses of apo GRX3 (52.7 kDa) and two molecules of apo BOLA2 (11.1 kDa) (Figure 5C). These results indicate that $[2Fe\text{-}2S]_2$ $GRX3_2$ interacts with apo BOLA2 to form, in the final protein mixture, a GRX3-$BOLA2_2$ heterotrimeric complex that binds $[2Fe\text{-}2S]^{2+}$ cluster(s). The EPR, UV−vis, CD, and analytical gel filtration data collected on this final mixture mirror the data previously obtained on a $[2Fe\text{-}2S]_2$ GRX3(GrxA/B)-$BOLA2_2$ complex produced by coexpressing human BOLA2 and GRX3(GrxA/B) in *E. coli* cells.[21] This indicates that the same type of cluster is bound to the heterotrimeric complex regardless of following different holo protein production approaches, i.e., chemical reconstitution vs *in vitro* and *in cell* Fe−S metalation, as well as different protein constructs, i.e. full-length protein vs a GrxA/GrxB domain construct.

Holo complex formation between $[2Fe\text{-}2S]_2$ $GRX3_2$ and apo BOLA2 was also followed by NMR, performing ^{1}H−^{15}N HSQC spectra on ^{15}N-labeled $[2Fe\text{-}2S]_2$ $GRX3_2$ titrated with unlabeled apo BOLA2 up to a protein−protein ratio of 1:4 and vice versa on ^{15}N-labeled BOLA2 titrated with unlabeled $[2Fe\text{-}2S]_2$ $GRX3_2$ up to a 4:1 protein−protein ratio. In the final mixture of the first titration, the NH signals of GRX3 affected by BOLA2 additions belong to residues of both Grx domains, while those of the Trx domain remain unperturbed. In the ^{1}H−^{15}N HSQC NMR spectra acquired throughout the titration steps (Figure 5D), a decrease in the intensity of some backbone NH signals of $[2Fe\text{-}2S]_2$ $GRX3_2$ (located more than 10 Å away from the paramagnetic $[2Fe\text{-}2S]^{2+}$ cluster and therefore only affected by BOLA2−GRX3 interaction) was observed, with the concomitant appearance of new backbone NH signals. This indicates the formation of a new species in solution in slow exchange, on the NMR time scale, with the $[2Fe\text{-}2S]_2$ $GRX3_2$ species (Figure 5D). This species has chemical shifts slightly different from those of the heterotrimeric complex formed by two apo BOLA2 molecules and an apo GRX3 molecule. In the final mixture, the NH signals of the $[2Fe\text{-}2S]_2$ $GRX3_2$ species fully disappeared in favor of the new NH signals, indicating the complete consumption of $[2Fe\text{-}2S]_2$ $GRX3_2$, which therefore completely evolves to the new species (Figure 5D). In the reverse titration, upon addition of unlabeled $[2Fe\text{-}2S]_2$ $GRX3_2$, some backbone NHs of ^{15}N-labeled BOLA2 broaden beyond detection, and others display chemical shift changes in a slow exchange regime on the NMR time scale (Figure 5D). The residues undergoing such spectral changes are essentially the same as those involved in the apo−apo interaction, indicating that the interaction region is the same in both apo and holo

DOI: 10.1021/jacs.5b10592
J. Am. Chem. Soc. 2015, 137, 16133−16143

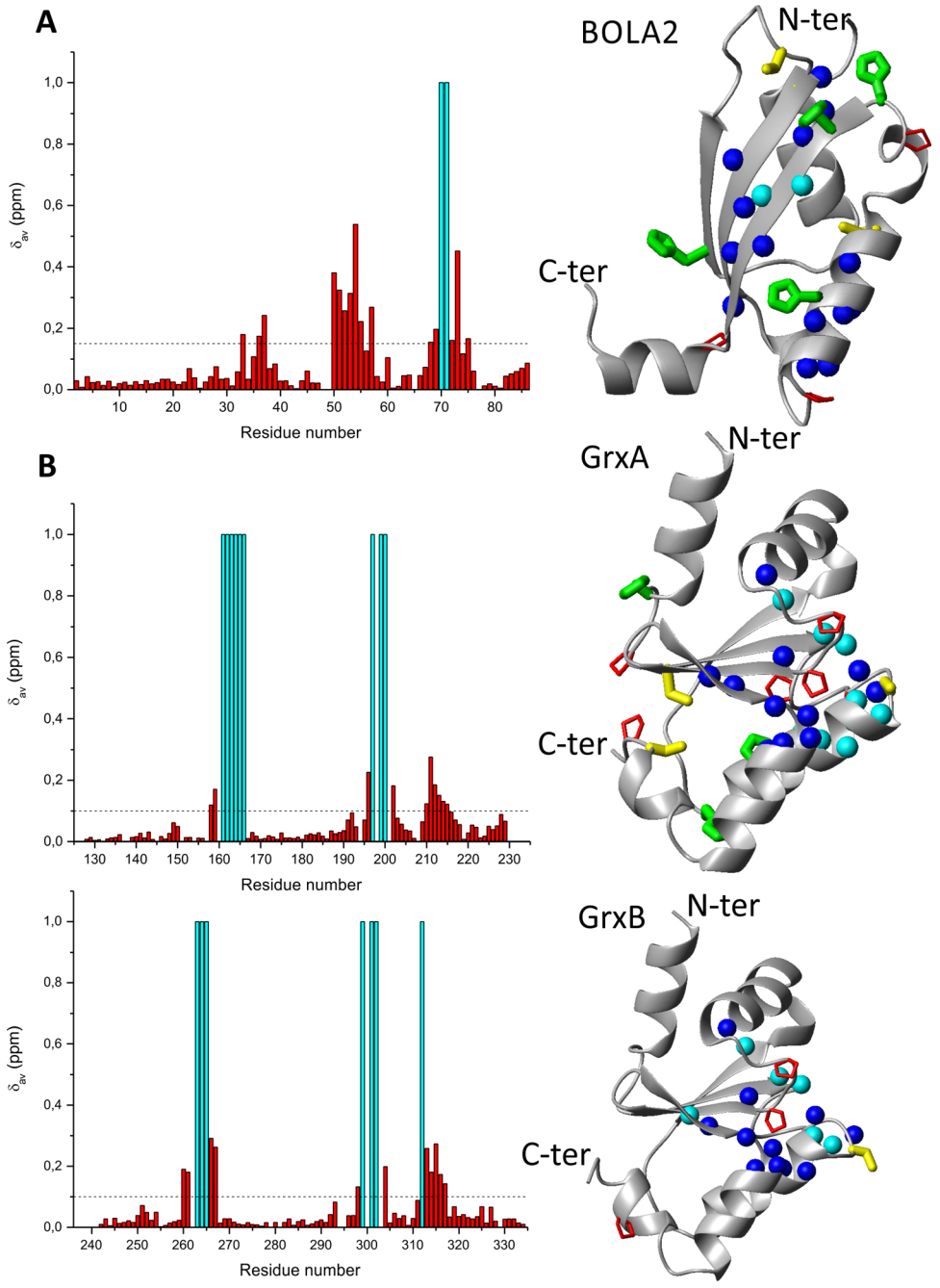

Figure 4. Mapping the interaction surfaces between BOLA2 and each GrxA and GrxB domain in the apo heterotrimeric complex. The left panels show backbone weighted average chemical shift differences δ_{av} for BOLA2 residues, observed upon addition of unlabeled apo GRX3(GrxA/B) to ^{15}N-labeled apo BOLA2 up to a 2:1 BOLA2-GRX3(GrxA/B) ratio (A) and for GRX3(GrxA/B) residues observed upon addition of 2 equiv of unlabeled apo BOLA2 to ^{15}N-labeled apo GRX3(GrxA/B) (B). A threshold of 0.15 ppm (mean value of δ_{av} plus 1σ, black dashed line) for BOLA2 and of 0.10 ppm for GRX3(GrxA/B) were used to identify significant chemical shift differences. Cyan bars identify residues whose backbone NHs broaden beyond detection upon complex formation. The δ_{av} value for Pro residues was arbitrarily set to zero. The right panels show backbone NHs experiencing significant chemical shift differences in the ^{1}H−^{15}N HSQC spectra upon the formation of the heterotrimeric apo GRX3(GrxA/B)-BOLA2$_2$ complex mapped as blue and cyan spheres on a structural model of apo BOLA2 (A) and on the crystal structure of GrxA (PDB ID 3ZYW) and GrxB (PDB ID 2YAN) domains of apo GRX3 (B). Blue spheres identify NHs showing significant chemical shift variations, and cyan spheres identify backbone NHs broaden beyond detection. Side-chains of His, Cys, and Pro residues are in green, yellow and red, respectively.

GRX3−BOLA2 interactions. Overall, the spectroscopic and gel filtration data indicate: (i) a complete conversion of the homodimeric [2Fe-2S]$_2$ GRX3$_2$ into a GRX3-BOLA2$_2$ heterotrimeric complex that contains [2Fe-2S]$^{2+}$ cluster(s); and (ii) similarly to what we found for the apo/apo heterotrimeric complex, the GrxA and GrxB domains of GRX3 interact with two BOLA2 molecules, while Trx domain is not involved in such interaction.

Two possible scenarios can occur at the 1:4 [2Fe-2S]$_2$ GRX3$_2$-BOLA2 ratio, i.e., the formation of a heterotrimeric GRX3-BOLA2$_2$ complex containing two [2Fe-2S]$^{2+}$ clusters together with the formation of a heterotrimeric apo GRX3-apo BOLA2$_2$ complex, or the formation of two heterotrimeric

DOI: 10.1021/jacs.5b10592
J. Am. Chem. Soc. 2015, 137, 16133−16143

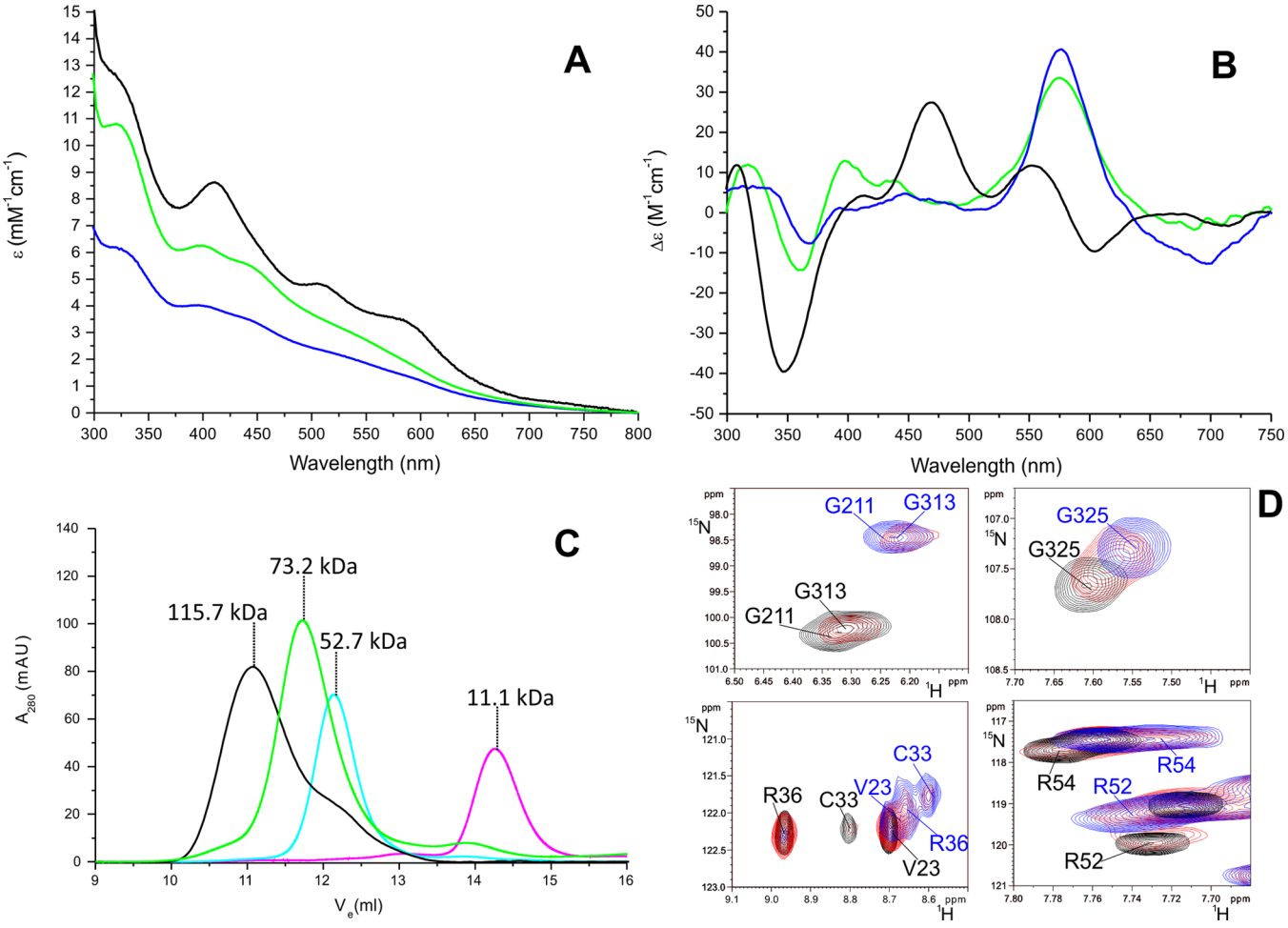

Figure 5. Formation of the [2Fe-2S] GRX3-BOLA2$_2$ complex from the interaction between [2Fe-2S]$_2$ GRX3$_2$ and apo BOLA2. (A) UV−vis and (B) CD spectra of [2Fe-2S]$_2$ GRX3$_2$ (black line), of the 1:4 [2Fe-2S]$_2$ GRX3$_2$-apo BOLA2 mixture (blue line), and of chemically reconstituted [2Fe-2S]$_2$ GRX3-BOLA2$_2$ (green line). (C) Analytical gel filtration (Superdex 75 HR 10/30 column) chromatograms of BOLA2 (magenta) and GRX3 (cyan) proteins in their apo states, of [2Fe-2S]$_2$ GRX3$_2$ complex (black), and of a 1:4 [2Fe-2S]$_2$ GRX3$_2$-apo BOLA2 mixture (green). The apparent molecular masses are reported at the top of each chromatographic peak. (D) In the upper panels, the overlay of ^{1}H−^{15}N HSQC spectral regions of ^{15}N-labeled [2Fe-2S]$_2$ GRX3$_2$ (black) and of 1:2 (red) and 1:4 (blue) ^{15}N-labeled [2Fe-2S]$_2$ GRX3$_2$/unlabeled apo BOLA2 mixtures. In the lower panels, the overlay of ^{1}H−^{15}N HSQC spectral regions of ^{15}N-labeled apo BOLA2 (black) and of 2:1 (red) and 4:1 (blue) ^{15}N-labeled apo BOLA2-unlabeled [2Fe-2S]$_2$ GRX3$_2$ mixtures.

GRX3-BOLA2$_2$ complexes each containing only one [2Fe-2S]$^{2+}$ cluster. The two scenarios result from two possible occurring molecular mechanisms, A and B shown in Scheme 1.

The key experimental evidence, that would allow us to provide information on whether a favorite mechanism between A and B is operative, is the detection of the formation of the apo free GRX3 form, which is observed indeed in the A mechanism only (Scheme 1). Analytical gel filtration was therefore performed on [2Fe-2S]$_2$ GRX3$_2$-apo BOLA2 protein mixtures at different protein:protein ratios, using a Superdex 75 HR 10/30 column to investigate the possible presence of free apo GRX3. These gel filtration analysis showed: (i) the presence of a main peak with an apparent molecular mass which increases from 68.0 to 73.2 kDa upon addition of apo BOLA2; (ii) the presence, only for [2Fe-2S]$_2$ GRX3$_2$-apo BOLA2 ratios >1:4, of a peak with the apparent molecular mass similar to that of apo BOLA2; and (iii) no formation of a peak with the apparent molecular mass of apo GRX3 at any investigated protein:protein ratio (Figure 6A).

The analytical gel filtration chromatography was also performed at higher resolution with a Superdex 200 10/300 increase column on protein mixtures at substoichiometric [2Fe-2S]$_2$ GRX3$_2$-apo BOLA2 ratios of 1:0.25, 1:0.5, and 1:1 (Figure 6B). It was observed the concurrent formation of (i) the 1:1 heterodimeric complex, corresponding to the peak with an apparent molecular mass of 71.3 kDa, which is indeed very close to the sum of the apparent molecular masses of one molecule of apo BOLA2 and one molecule of apo GRX3 (i.e., 70.4 kDa), and (ii) of the heterotrimeric complex, corresponding to the peak with an apparent molecular mass of 87.4 kDa, which is indeed close to the sum of the apparent molecular masses of two apo BOLA2 molecules and one molecule of apo GRX3 (i.e., 82.0 kDa). The peak of apo GRX3, which is always present at a low percentage in the chemically reconstituted [2Fe-2S]$_2$ GRX3$_2$ sample, does not increase in its intensity upon BOLA2 substoichiometric additions (Figure 6B), as expected if the A mechanism was the favored process. From these gel filtration data we therefore conclude that the B mechanism is the preferential occurring process.

[2Fe-2S]$_2$ GRX3-BOLA2$_2$ Complex Transfers [2Fe-2S]$^{2+}$ Clusters to apo Anamorsin. Cluster transfer from [2Fe-2S]$_2$ GRX3-BOLA2$_2$ to apo anamorsin was followed by UV−vis, CD

DOI: 10.1021/jacs.5b10592
J. Am. Chem. Soc. 2015, 137, 16133−16143

Scheme 1. Possible Solution Equilibria upon Reaction of $[2Fe\text{-}2S]_2$ $GRX3_2$ With apo BOLA2 up to a 1:4 Ratio[a]

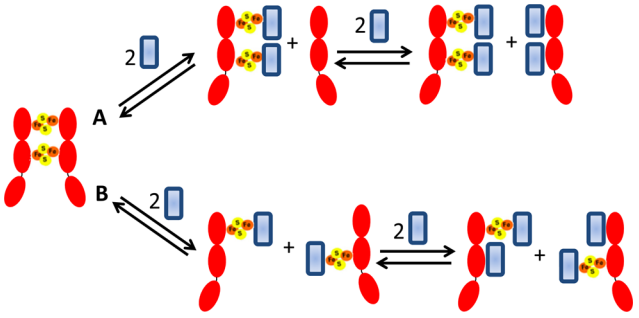

[a](A) Two molecules of apo BOLA2 (in blue) interact with a $[2Fe\text{-}2S]_2$ $GRX3_2$ molecule (GRX3 molecules are in red) to form a heterotrimeric GRX3-$BOLA2_2$ complex that binds two $[2Fe\text{-}2S]^{2+}$ clusters and an apo GRX3 molecule. The further addition of 2 equiv of apo BOLA2 determines the formation of an apo heterotrimeric GRX3-$BOLA2_2$ complex. (B) Two distinct heterodimeric GRX3-BOLA2 complexes, containing one $[2Fe\text{-}2S]^{2+}$ cluster each, are first formed. Then, the further addition of 2 equiv of apo BOLA2 determines the formation of two distinct heterotrimeric GRX3-$BOLA2_2$ complexes still containing one $[2Fe\text{-}2S]^{2+}$ cluster each.

spectroscopy, and analytical gel filtration. Once the chemically reconstituted $[2Fe\text{-}2S]_2$ GRX3-$BOLA2_2$ heterotrimeric complex was titrated with apo anamorsin up to a 1:1 protein–protein ratio, in the UV–vis and CD spectra the absorbance peaks typical of $[2Fe\text{-}2S]_2$ GRX3-$BOLA2_2$ disappeared and the absorbance peaks typical of the $[2Fe\text{-}2S]^{2+}$ cluster-bound form of anamorsin ($[2Fe\text{-}2S]$ anamorsin)[29,33] appeared (Figure 7A,B). The CD spectrum of the final 1:1 mixture essentially corresponds to that of $[2Fe\text{-}2S]$ anamorsin, being clearly distinguishable from that of $[2Fe\text{-}2S]_2$ GRX3-$BOLA2_2$. Analytical gel filtration chromatography performed with Superdex 75 HR 10/30 column on the final 1:1 mixture showed the presence of a main peak with an apparent molecular mass of 128.2 kDa, which essentially corresponds to the sum of the apparent molecular masses of $[2Fe\text{-}2S]_2$ GRX3-$BOLA2_2$ (73.2 kDa) and apo anamorsin (52.0 kDa) (Figure 7C). Overall, the data showed that (i) both $[2Fe\text{-}2S]^{2+}$ cluster are completely transferred from $[2Fe\text{-}2S]_2$ GRX3-$BOLA2_2$ to apo anamorsin and (ii) the final product is a complex formed by an apo GRX3 molecule, two apo BOLA2 molecules and a $[2Fe\text{-}2S]$ anamorsin molecule (GRX3-$BOLA2_2$-$[2Fe\text{-}2S]$ anamorsin, hereafter).

Moreover, by gel filtrating a 1:1 mixture of apo GRX3(GrxA/B)-$BOLA2_2$ and $[2Fe\text{-}2S]$ anamorsin, a peak corresponding to a ternary complex formed by GRX3(GrxA/B), BOLA2, and anamorsin is not observed (Supporting Information Figure S4), at variance to what detected in the 1:1 GRX3-$BOLA2_2$-$[2Fe\text{-}2S]$ anamorsin mixture, where the corresponding ternary complex is formed (Figure 7C). This demonstrates that, in the final GRX3-$BOLA2_2$-$[2Fe\text{-}2S]$ anamorsin complex, the interaction between apo GRX3–$BOLA2_2$ and $[2Fe\text{-}2S]$ anamorsin depends on the presence of the Trx domain of GRX3. We had previously shown that the Trx domain of GRX3 interacts with the N-terminal domain of anamorsin mediating the cluster transfer between the two proteins.[24] Here we show that the Trx domain, in addition of being essential for the complex formation between anamorsin and GRX3-$BOLA2_2$ in the GRX3-$BOLA2_2$-$[2Fe\text{-}2S]$ anamorsin complex, maintains the same conformational freedom as it has in the homodimeric $[2Fe\text{-}2S]_2$ $GRX3_2$ complex. Therefore, we propose that the cluster transfer mechanism previously reported for $[2Fe\text{-}2S]_2$ $GRX3_2$[24] is also operative in the $[2Fe\text{-}2S]_2$ GRX3–$BOLA2_2$-apo anamorsin interaction, i.e., the protein recognition, specifically occurring between the N-terminal domains of the two proteins, plays a role in the cluster transfer process.

DISCUSSION

BolA-like proteins have recently emerged as novel players in iron metabolism, being involved, on the basis of genetic and biochemical studies, in intracellular iron regulation pathways and in the maturation of Fe/S cluster-containing proteins.[3,17,34] Specifically, a role for the cytosolic *S. cerevisiae* BolA2 (usually

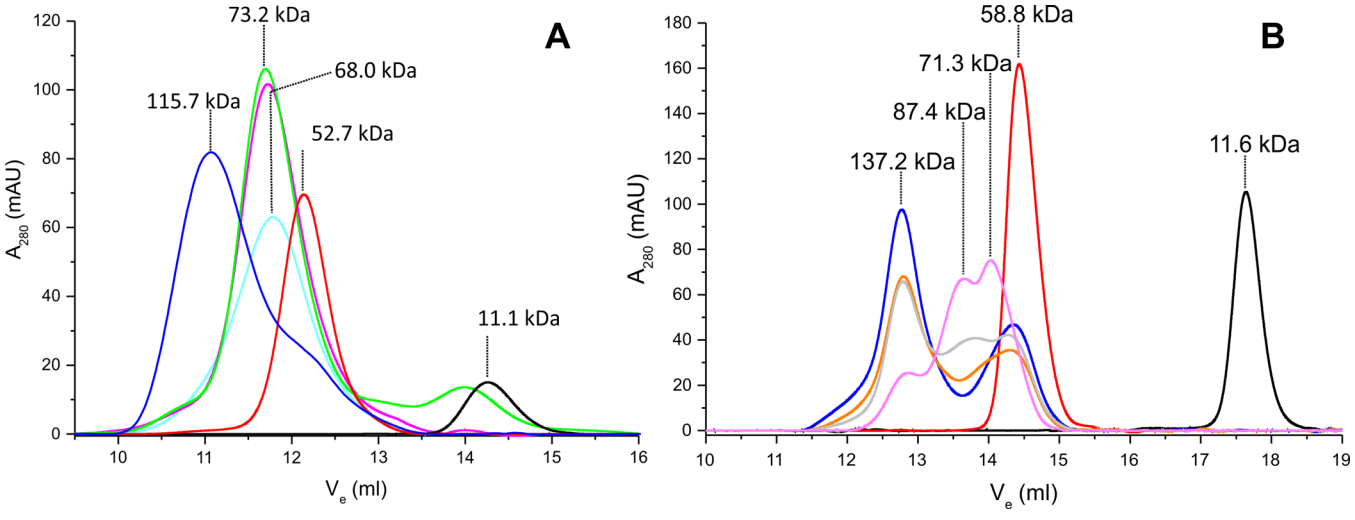

Figure 6. The formation of apo GRX3 is not observed upon the interaction of $[2Fe\text{-}2S]_2$ $GRX3_2$ with apo BOLA2. Analytical gel filtration chromatograms of (A) BOLA2 (black) and GRX3 (red) proteins in their apo states, of $[2Fe\text{-}2S]_2$ $GRX3_2$ (blue) and of a 1:2 (cyan), 1:4 (magenta), 1:6 (green) $[2Fe\text{-}2S]_2$ $GRX3_2$-apo BOLA2 mixtures (Superdex 75 HR 10/30 column), and of (B) BOLA2 (black) and GRX3 (red) proteins in their apo states, of $[2Fe\text{-}2S]_2$ $GRX3_2$ (blue) and of a 1:0.25 (orange), 1:0.5 (light gray), 1:1 (light magenta) $[2Fe\text{-}2S]_2$ $GRX3_2$-apo BOLA2 mixtures (Superdex 200 10/300 increase column). The apparent molecular masses are reported at the top of each chromatographic peak.

DOI: 10.1021/jacs.5b10592
J. Am. Chem. Soc. 2015, 137, 16133–16143

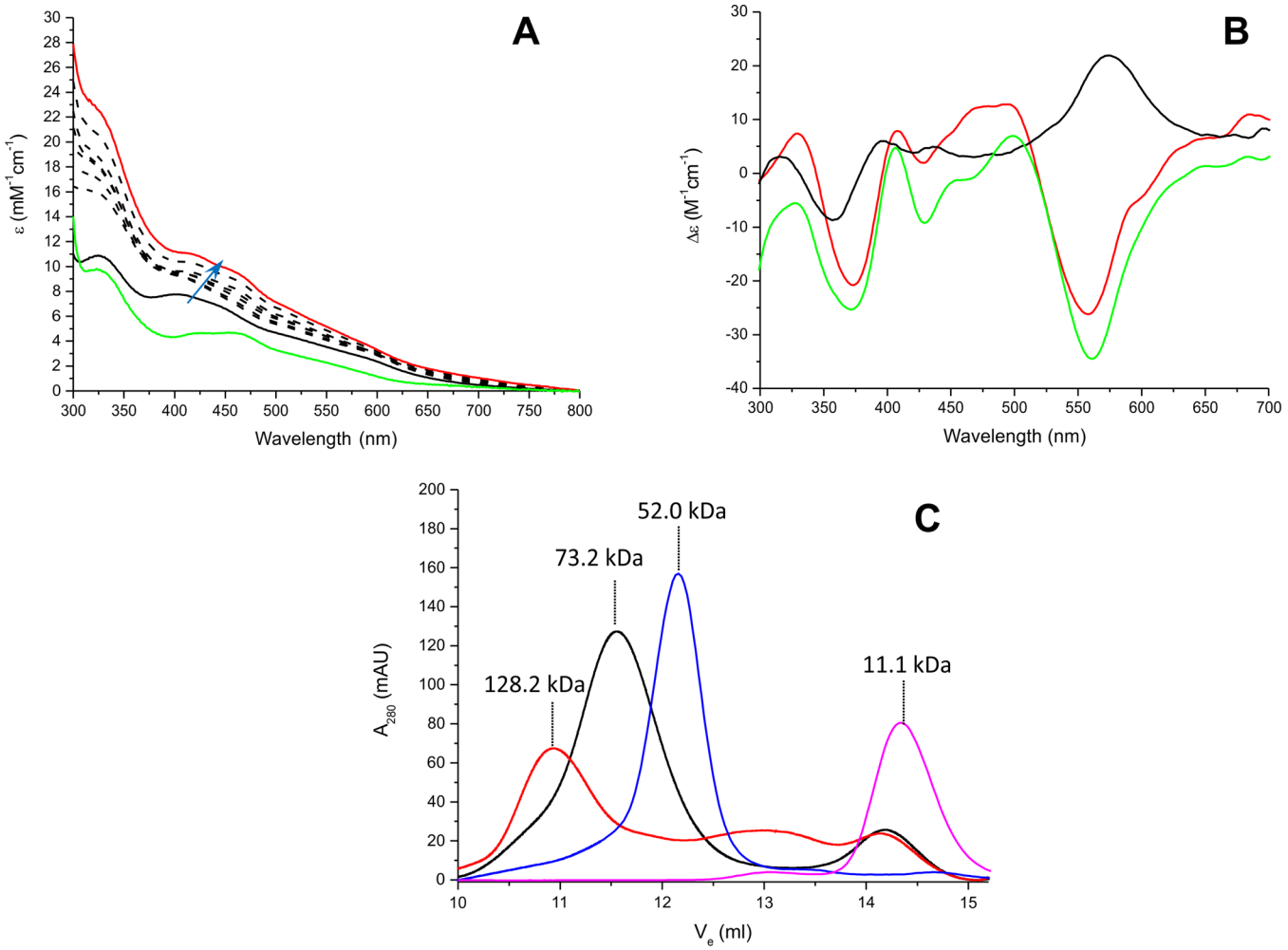

Figure 7. $[2Fe\text{-}2S]_2$ GRX3-BOLA2$_2$ transfers its clusters to apo anamorsin upon complex formation. (A) UV−vis spectra of $[2Fe\text{-}2S]_2$ GRX3-BOLA2$_2$ (black line) titrated with 0.1, 0.2, 0.3, 0.4, 0.5, 0.6, 0.8 equiv of apo anamorsin (black dashed lines). The arrow indicates the direction of the change in intensity and wavelength of the absorbance peaks with the increase of apo anamorsin concentration. The UV−vis spectra of the final 1:1 protein mixture and of $[2Fe\text{-}2S]$ anamorsin are shown as red and green lines, respectively. (B) CD spectra acquired to follow cluster transfer from $[2Fe\text{-}2S]_2$ GRX3-BOLA2$_2$ to apo anamorsin. Black line: chemically reconstituted $[2Fe\text{-}2S]_2$ GRX3-BOLA2$_2$; green line: $[2Fe\text{-}2S]$ anamorsin; red line: 1:1 mixture of $[2Fe\text{-}2S]_2$ GRX3-BOLA2$_2$ and apo anamorsin. (C) Analytical gel filtration (75 HR 10/30 column) chromatograms of BOLA2 (magenta) and anamorsin (blue) proteins in their apo states, of $[2Fe\text{-}2S]_2$ GRX3-BOLA2$_2$ (black), and of a 1:1 mixture between $[2Fe\text{-}2S]_2$ GRX3-BOLA2$_2$ and apo anamorsin (red). The apparent molecular masses are reported at the top of each chromatographic peak.

named Fra2) in iron regulation[14,16,35] and for the mitochondrial human BOLA3 in the production of the lipoate-containing 2-oxoacid dehydrogenases and in the assembly of the respiratory chain complexes[36] has been established. However, there are no studies exploring analogous functions for BolA homologues in *S. cerevisiae* and humans. In particular, since the Fra2-dependent, iron signaling pathway described in *S. cerevisiae* is not conserved in humans,[27] a homologous regulatory function of BOLA2 in human cells can be excluded.

In this work we have investigated by *in vitro* studies the role of the GRX3−BOLA2 interaction in cytoplasmic Fe/S protein biogenesis, i.e., in the CIA pathway, being inspired (i) by the general accepted view that BOLA2 protein is involved in human iron metabolism once interacting with its protein partner GRX3;[17,37] (ii) by knowing that human BOLA2 forms *in vitro* a $[2Fe\text{-}2S]$-bridged hetero complex with each monothiol Grx domain of GRX3;[21] and (iii) by our recent finding that the holo form of GRX3 is capable to mature the cytosolic Fe/S protein anamorsin, thus proposing GRX3 as a component of the CIA machinery.[24]

Our data showed that apo BOLA2 and the Grx domains of apo GRX3 significantly and specifically interact forming an apo heterotrimeric complex composed by a GRX3 molecule and two BOLA2 molecules. This complex is able to bind two $[2Fe\text{-}2S]^{2+}$ clusters upon chemical reconstitution. The same cluster content was achieved in the heterotrimeric complex obtained by co-expressing in *E. coli* cells human BOLA2 and a construct of GRX3 containing only the two Grx domains.[21] A heterotrimeric GRX3-BOLA2$_2$ complex was also obtained by mixing *in vitro* $[2Fe\text{-}2S]_2$ GRX3$_2$ with apo BOLA2. However, in this case the formed heterotrimeric GRX3-BOLA2$_2$ complex contains only one $[2Fe\text{-}2S]^{2+}$ cluster per complex. These data indicate that a heterotrimeric GRX3-BOLA2$_2$ complex containing two $[2Fe\text{-}2S]^{2+}$ clusters can be formed in one-step process only by inserting two $[2Fe\text{-}2S]^{2+}$ clusters in an apo heterotrimeric GRX3-BOLA2$_2$ complex. Therefore, it is reasonable to suggest that the apo heterotrimeric GRX3-BOLA2$_2$ complex, similarly to apo GRX3 alone,[24] might be a physiologically relevant species that receives two $[2Fe\text{-}2S]^{2+}$ clusters in the cytoplasm from a still unknown protein partner.

DOI: 10.1021/jacs.5b10592
J. Am. Chem. Soc. 2015, 137, 16133−16143

In support of this, our data showed that, similarly to what observed for the holo homodimeric form of GRX3 containing two $[2Fe\text{-}2S]^{2+}$ clusters,[24] the heterotrimeric complex containing two $[2Fe\text{-}2S]^{2+}$ clusters matures the CIA machinery component anamorsin by transferring both clusters to the CIAPIN1 domain of apo anamorsin to generate [2Fe-2S] anamorsin. Both complexes, i.e., the homodimeric GRX3 and the heterotrimeric GRX3-BOLA2$_2$ complexes containing two $[2Fe\text{-}2S]^{2+}$ clusters, can thus be active players, at the cellular level, for maturing anamorsin. The present data also suggest that the mechanism of cluster transfer relying on the interaction between the N-terminal domains of anamorsin and GRX3[24] is common to both cluster transfer processes, i.e., from $[2Fe\text{-}2S]_2$ GRX3$_2$ to apo anamorsin and from $[2Fe\text{-}2S]_2$ GRX3-BOLA2$_2$ to apo anamorsin.

Now, the arising question is whether and how the cells can select the homodimeric $[2Fe\text{-}2S]_2$ GRX3$_2$ vs the heterotrimeric $[2Fe\text{-}2S]_2$ GRX3-BOLA2$_2$ complex to mature anamorsin. Assuming that the interaction between apo BOLA2 and apo GRX3 is physiologically relevant, the relative cellular levels of GRX3 and BOLA2, which can be regulated by cellular conditions (i.e., aerobic vs anaerobic cellular growth, oxidative stress, etc.), should select which of the two complexes mature anamorsin. The sensitivity of Fe/S protein biogenesis pathways toward oxygen and/or oxidative stress has been observed for members of both bacterial and eukaryotic Fe/S cluster assembly machineries.[38−42] Recently, two new CIA yeast proteins were found to be specifically involved in the maturation of the ribosome-associated ABC protein Rli1, and this function is fundamental under oxidative stress cellular conditions, as in the absence of oxygen these factors can be overcome to some extent without losing cell viability.[43] It might be possible therefore that the homodimeric $[2Fe\text{-}2S]_2$ GRX3$_2$ complex is operative in normal cellular conditions, while the heterotrimeric $[2Fe\text{-}2S]_2$ GRX3-BOLA2$_2$ complex works under oxidative stress. Consistently with this possible model, bacterial BolA proteins have been observed to be specifically required under aerobic and oxidative stress conditions. For instance, in *E. coli* BolA protein is upregulated under oxidative stress conditions,[44] and in bacterial operons, BolA tends to occur not only with a monothiol glutaredoxin, but also with proteins involved in defense against oxidative stress.[45] Also in eukaryotic genomes, the presence of BOLAs strongly correlates with an aerobic metabolism.[46] Last but not least, $[2Fe\text{-}2S]_2$ GRX3-BOLA2$_2$ complex is stable in air, while the homodimeric $[2Fe\text{-}2S]_2$ GRX3$_2$ is oxidatively labile and is gradually degraded in air over a period of ∼1 h.[21] Thus, BOLA2 binding to GRX3 stabilizes $[2Fe\text{-}2S]^{2+}$ clusters against oxidative degradation, similarly to what was observed in the yeast $[2Fe\text{-}2S]^{2+}$ Fra2-Grx3/4 complexes.[11]

CONCLUSION

In conclusion, we propose that the GRX3−BOLA2 interaction might have a role in the CIA pathway. GRX3 and BOLA2 form indeed an apo complex composed by two molecules of BOLA2 bound to a molecule of GRX3. This species, upon binding two $[2Fe\text{-}2S]^{2+}$ clusters, is able to transfer both of them to anamorsin, thus maturing it in one-step process, similarly to what we already showed for the holo homodimeric GRX3 form.[24] The $[2Fe\text{-}2S]^{2+}$ cluster bound forms of GRX3 and GRX3-BOLA2$_2$ might thus act as $[2Fe\text{-}2S]^{2+}$ cluster transfer components in the cytosol, in a similar way as monothiol glutaredoxins do in mitochondria.[7,19,47,48]

ASSOCIATED CONTENT

Supporting Information

The Supporting Information is available free of charge on the ACS Publications website at DOI: 10.1021/jacs.5b10592.

Four figures reporting: ^{15}N backbone amide relaxation parameters of apo BOLA2; an overlay of $^{1}H-^{15}N$ HSQC spectra of different constructs of apo GRX3 in the presence or absence of apo BOLA2; EPR spectra of $[2Fe\text{-}2S]_2$ GRX3-BOLA2$_2$ complexes obtained by chemical reconstitution and by mixing $[2Fe\text{-}2S]_2$ GRX3$_2$ with apo BOLA2; gel filtration of a 1:1 mixture of apo GRX3(GrxA/B)-BOLA2$_2$ and [2Fe-2S] anamorsin (PDF)

AUTHOR INFORMATION

Corresponding Authors

*banci@cerm.unifi.it

*ciofi@cerm.unifi.it

Notes

The authors declare no competing financial interest.

ACKNOWLEDGMENTS

We thank Angelo Gallo (CERM) for assistance in recording the EPR spectra. This work was supported by Ente Cassa di Risparmio (grant ID no. 2013/7201) and by the European Integrated Structural Biology Infrastructure (INSTRUCT), which is part of the European Strategy Forum on Research Infrastructures and supported by national member subscriptions.

REFERENCES

(1) Lill, R. *Nature* **2009**, *460*, 831−838.

(2) Herrero, E.; de la Torre-Ruiz, M. A. *Cell. Mol. Life Sci.* **2007**, *64*, 1518−1530.

(3) Couturier, J.; Przybyla-Toscano, J.; Roret, T.; Didierjean, C.; Rouhier, N. *Biochim. Biophys. Acta, Mol. Cell Res.* **2015**, *1853*, 1513−1527.

(4) Rouhier, N.; Couturier, J.; Johnson, M. K.; Jacquot, J. P. *Trends Biochem. Sci.* **2010**, *35*, 43−52.

(5) Picciocchi, A.; Saguez, C.; Boussac, A.; Cassier-Chauvat, C.; Chauvat, F. *Biochemistry* **2007**, *46*, 15018−15026.

(6) Johansson, C.; Roos, A. K.; Montano, S. J.; Sengupta, R.; Filippakopoulos, P.; Guo, K.; von Delft, F.; Holmgren, A.; Oppermann, U.; Kavanagh, K. L. *Biochem. J.* **2011**, *433*, 303−311.

(7) Uzarska, M. A.; Dutkiewicz, R.; Freibert, S. A.; Lill, R.; Muhlenhoff, U. *Mol. Biol. Cell* **2013**, *24*, 1830−1841.

(8) Muhlenhoff, U.; Gerber, J.; Richhardt, N.; Lill, R. *EMBO J.* **2003**, *22*, 4815−4825.

(9) Muhlenhoff, U.; Molik, S.; Godoy, J. R.; Uzarska, M. A.; Richter, N.; Seubert, A.; Zhang, Y.; Stubbe, J.; Pierrel, F.; Herrero, E.; Lillig, C. H.; Lill, R. *Cell Metab.* **2010**, *12*, 373−385.

(10) Hoffmann, B.; Uzarska, M. A.; Berndt, C.; Godoy, J. R.; Haunhorst, P.; Lillig, C. H.; Lill, R.; Muhlenhoff, U. *Antioxid. Redox Signaling* **2011**, *15*, 19−30.

(11) Li, H.; Mapolelo, D. T.; Dingra, N. N.; Naik, S. G.; Lees, N. S.; Hoffman, B. M.; Riggs-Gelasco, P. J.; Huynh, B. H.; Johnson, M. K.; Outten, C. E. *Biochemistry* **2009**, *48*, 9569−9581.

(12) Ojeda, L.; Keller, G.; Muhlenhoff, U.; Rutherford, J. C.; Lill, R.; Winge, D. R. *J. Biol. Chem.* **2006**, *281*, 17661−17669.

(13) Pujol-Carrion, N.; Belli, G.; Herrero, E.; Nogues, A.; de la Torre-Ruiz, M. A. *J. Cell Sci.* **2006**, *119*, 4554−4564.

(14) Kumanovics, A.; Chen, O. S.; Li, L.; Bagley, D.; Adkins, E. M.; Lin, H.; Dingra, N. N.; Outten, C. E.; Keller, G.; Winge, D.; Ward, D. M.; Kaplan, J. *J. Biol. Chem.* **2008**, *283*, 10276−10286.

DOI: 10.1021/jacs.5b10592
J. Am. Chem. Soc. 2015, 137, 16133−16143

(15) Li, H.; Mapolelo, D. T.; Dingra, N. N.; Keller, G.; Riggs-Gelasco, P. J.; Winge, D. R.; Johnson, M. K.; Outten, C. E. *J. Biol. Chem.* **2011**, *286*, 867−876.
(16) Poor, C. B.; Wegner, S. V.; Li, H.; Dlouhy, A. C.; Schuermann, J. P.; Sanishvili, R.; Hinshaw, J. R.; Riggs-Gelasco, P. J.; Outten, C. E.; He, C. *Proc. Natl. Acad. Sci. U. S. A.* **2014**, *111*, 4043−4048.
(17) Li, H.; Outten, C. E. *Biochemistry* **2012**, *51*, 4377−4389.
(18) Vilella, F.; Alves, R.; Rodriguez-Manzaneque, M. T.; Belli, G.; Swaminathan, S.; Sunnerhagen, P.; Herrero, E. *Comp. Funct. Genomics* **2004**, *5*, 328−341.
(19) Banci, L.; Brancaccio, D.; Ciofi-Baffoni, S.; Del Conte, R.; Gadepalli, R.; Mikolajczyk, M.; Neri, S.; Piccioli, M.; Winkelmann, J. *Proc. Natl. Acad. Sci. U. S. A.* **2014**, *111*, 6203−6208.
(20) Lill, R.; Hoffmann, B.; Molik, S.; Pierik, A. J.; Rietzschel, N.; Stehling, O.; Uzarska, M. A.; Webert, H.; Wilbrecht, C.; Muhlenhoff, U. *Biochim. Biophys. Acta, Mol. Cell Res.* **2012**, *1823*, 1491−1508.
(21) Li, H.; Mapolelo, D. T.; Randeniya, S.; Johnson, M. K.; Outten, C. E. *Biochemistry* **2012**, *51*, 1687−1696.
(22) Haunhorst, P.; Berndt, C.; Eitner, S.; Godoy, J. R.; Lillig, C. H. *Biochem. Biophys. Res. Commun.* **2010**, *394*, 372−376.
(23) Haunhorst, P.; Hanschmann, E. M.; Brautigam, L.; Stehling, O.; Hoffmann, B.; Muhlenhoff, U.; Lill, R.; Berndt, C.; Lillig, C. H. *Mol. Biol. Cell* **2013**, *24*, 1895−1903.
(24) Banci, L.; Ciofi-Baffoni, S.; Gajda, K.; Muzzioli, R.; Peruzzini, R.; Winkelmann, J. *Nat. Chem. Biol.* **2015**, *11*, 772−778.
(25) Lill, R.; Dutkiewicz, R.; Freibert, S. A.; Heidenreich, T.; Mascarenhas, J.; Netz, D. J.; Paul, V. D.; Pierik, A. J.; Richter, N.; Stumpfig, M.; Srinivasan, V.; Stehling, O.; Muhlenhoff, U. *Eur. J. Cell Biol.* **2015**, *94*, 280−291.
(26) Paul, V. D.; Lill, R. *Biochim. Biophys. Acta, Mol. Cell Res.* **2015**, *1853*, 1528−1539.
(27) Rouault, T. A. *Nat. Chem. Biol.* **2006**, *2*, 406−414.
(28) Cheng, N. H.; Zhang, W.; Chen, W. Q.; Jin, J.; Cui, X.; Butte, N. F.; Chan, L.; Hirschi, K. D. *FEBS J.* **2011**, *278*, 2525−2539.
(29) Banci, L.; Bertini, I.; Ciofi-Baffoni, S.; Boscaro, F.; Chatzi, A.; Mikolajczyk, M.; Tokatlidis, K.; Winkelmann, J. *Chem. Biol.* **2011**, *18*, 794−804.
(30) Lian, L. Y.; Roberts, G. C. K. *NMR of Macromolecules. A Practical Approach*; Oxford University Press: Oxford, 1993; pp 153−182.
(31) Williamson, M. P. *Prog. Nucl. Magn. Reson. Spectrosc.* **2013**, *73*, 1−16.
(32) Kasai, T.; Inoue, M.; Koshiba, S.; Yabuki, T.; Aoki, M.; Nunokawa, E.; Seki, E.; Matsuda, T.; Matsuda, N.; Tomo, Y.; Shirouzu, M.; Terada, T.; Obayashi, N.; Hamana, H.; Shinya, N.; Tatsuguchi, A.; Yasuda, S.; Yoshida, M.; Hirota, H.; Matsuo, Y.; Tani, K.; Suzuki, H.; Arakawa, T.; Carninci, P.; Kawai, J.; Hayashizaki, Y.; Kigawa, T.; Yokoyama, S. *Protein Sci.* **2004**, *13*, 545−548.
(33) Banci, L.; Ciofi-Baffoni, S.; Mikolajczyk, M.; Winkelmann, J.; Bill, E.; Pandelia, M. E. *JBIC, J. Biol. Inorg. Chem.* **2013**, *18*, 883−893.
(34) Dhalleine, T.; Rouhier, N.; Couturier, J. *Plant Signaling Behav.* **2014**, *9*, e28564.
(35) Lesuisse, E.; Knight, S. A.; Courel, M.; Santos, R.; Camadro, J. M.; Dancis, A. *Genetics* **2005**, *169*, 107−122.
(36) Cameron, J. M.; Janer, A.; Levandovskiy, V.; MacKay, N.; Rouault, T. A.; Tong, W. H.; Ogilvie, I.; Shoubridge, E. A.; Robinson, B. H. *Am. J. Hum. Genet.* **2011**, *89*, 486−495.
(37) Couturier, J.; Przybyla-Toscano, J.; Roret, T.; Didierjean, C.; Rouhier, N. *Biochim. Biophys. Acta, Mol. Cell Res.* **2015**, *1853*, 1513−1527.
(38) Johnson, D. C.; Unciuleac, M. C.; Dean, D. R. *J. Bacteriol.* **2006**, *188*, 7551−7561.
(39) Tan, G.; Lu, J.; Bitoun, J. P.; Huang, H.; Ding, H. *Biochem. J.* **2009**, *420*, 463−472.
(40) Angelini, S.; Gerez, C.; Ollagnier-de, C. S.; Sanakis, Y.; Fontecave, M.; Barras, F.; Py, B. *J. Biol. Chem.* **2008**, *283*, 14084−14091.
(41) Bandyopadhyay, S.; Naik, S. G.; O'Carroll, I. P.; Huynh, B. H.; Dean, D. R.; Johnson, M. K.; Dos Santos, P. C. *J. Biol. Chem.* **2008**, *283*, 14092−14099.
(42) Py, B.; Gerez, C.; Angelini, S.; Planel, R.; Vinella, D.; Loiseau, L.; Talla, E.; Brochier-Armanet, C.; Garcia, S. R.; Latour, J. M.; Ollagnier-de, C. S.; Fontecave, M.; Barras, F. *Mol. Microbiol.* **2012**, *86*, 155−171.
(43) Paul, V. D.; Muhlenhoff, U.; Stumpfig, M.; Seebacher, J.; Kugler, K. G.; Renicke, C.; Taxis, C.; Gavin, A. C.; Pierik, A. J.; Lill, R. *eLife* **2015**, *4*, e08231.
(44) Santos, J. M.; Freire, P.; Vicente, M.; Arraiano, C. M. *Mol. Microbiol.* **1999**, *32*, 789−798.
(45) Huynen, M. A.; Spronk, C. A.; Gabaldon, T.; Snel, B. *FEBS Lett.* **2005**, *579*, 591−596.
(46) Willems, P.; Wanschers, B. F.; Esseling, J.; Szklarczyk, R.; Kudla, U.; Duarte, I.; Forkink, M.; Nooteboom, M.; Swarts, H.; Gloerich, J.; Nijtmans, L.; Koopman, W.; Huynen, M. A. *Antioxid. Redox Signaling* **2013**, *18*, 129−138.
(47) Brancaccio, D.; Gallo, A.; Mikolajczyk, M.; Zovo, K.; Palumaa, P.; Novellino, E.; Piccioli, M.; Ciofi-Baffoni, S.; Banci, L. *J. Am. Chem. Soc.* **2014**, *136*, 16240−16250.
(48) Muhlenhoff, U.; Gerber, J.; Richhardt, N.; Lill, R. *EMBO J.* **2003**, *22*, 4815−4825.

DOI: 10.1021/jacs.5b10592
J. Am. Chem. Soc. 2015, 137, 16133−16143